

Joint Phase Noise Estimation and Data Detection in Coded MIMO Systems

Arif O. Isikman[†], Hani Mehrpouyan[‡], *Member, IEEE*, Ali A. Nasir[‡], *Member, IEEE*, Alexander G. Amat[†], *Senior Member, IEEE*, and Rodney A. Kennedy[‡], *Fellow, IEEE*.

[†]Communications Systems Group at Chalmers University of Technology, Sweden,

[‡]Department of ECE at California State University, Bakersfield, USA,

[‡]The Research School of Engineering at the Australian National University, Australia.

{Emails: isikman@student.chalmers.se, hani.mehr@ieee.org, ali.nasir@anu.edu.au, alexandre.graell@chalmers.se, and rodney.kennedy@anu.edu.au}

Abstract

In this paper, the problem of joint oscillator *phase noise (PHN)* estimation and data detection for *multi-input multi-output (MIMO)* systems using *bit-interleaved coded modulation (BICM)* is analyzed. A new MIMO receiver that iterates between the estimator and the detector, based on the *expectation-maximization (EM)* framework, is proposed. It is shown that at high signal-to-noise ratios, a *maximum a posteriori estimator (MAP)* can be used to carry out the maximization step of the EM algorithm. Moreover, to reduce the computational complexity of the proposed EM algorithm, a soft decision-directed *extended Kalman filter-smoother (EKFS)* is applied instead of the MAP estimator to track the PHN parameters. Numerical results show that by combining the proposed EKFS based approach with an iterative detector that employs *low density parity check (LDPC)* codes, PHN can be accurately tracked. Simulations also demonstrate that compared to existing algorithms, the proposed iterative receiver can significantly enhance the performance of MIMO systems in the presence of PHN.

Index Terms

Multi-input multi-output (MIMO), phase noise (PHN), joint phase noise estimation and data detection, bit-interleaved-coded-modulation (BICM).

This work is part of the first author's Master dissertation, which was completed at Chalmers University of Technology and Ericsson AB [1]. This research was supported by Swedish research foundation Vinnova and the Australian Research Council's Discovery Project funding scheme (project number DP110102548).

I. INTRODUCTION

A. Motivation and Literature Survey

It is well-known that *multi-input multi-output (MIMO)* technology allows for more efficient use of the available spectrum [2]. To this end, *bit-interleaved-coded-modulation (BICM)* is a popular scheme that enables communication systems to fully exploit the spectrum efficiency promised by MIMO technology [3]. However, the performance of MIMO systems degrades dramatically in the presence of synchronization errors. In fact, one of the main limiting factors in the deployment of MIMO systems in microwave links, e.g., for establishing the backhaul link, is *phase noise (PHN)* [4].

Analogous to other circuits, the oscillator circuitry is affected by thermal noise. As such, the output of practical oscillators is not perfectly periodic and is affected by PHN. PHN interacts with the transmitted symbols in a non-linear manner and significantly distorts the received signal [5]. Moreover, due to its time varying nature [6], it is difficult to accurately track and compensate the deteriorating effect of PHN at the receiver.

It is well-known that parameter estimation accuracy can be significantly enhanced if it is carried out jointly with data detection [7]. As such, many iterative receiver structures have been proposed that utilize forward error correcting (FEC) codes to perform joint synchronization parameter estimation and data detection. Such iterative receivers were first proposed in [8] and have since been formalized in [9] with the use of the *expectation-maximization (EM)* framework. In [10], a coded iterative structure based on the EM algorithm for tracking PHN in single-input single-output (SISO) systems is proposed. However, the performance of the approach in [10] degrades with increasing block length and it is also not applicable to MIMO systems. Code-aided synchronization based on the EM framework for joint channel estimation and frequency/time synchronization for MIMO systems is considered in [11]. However, in [11], the synchronization parameters are assumed to be constant and deterministic over the length of a block, which is not a valid assumption for time varying PHN. It is also important to note that unlike SISO systems, MIMO systems may need to employ independent oscillators at each transmit and receive antennas, e.g., for *line-of-sight (LoS)* MIMO systems, where the antennas are positioned far apart from one another [6], [12]¹ or in the case of multi-user MIMO systems, where independent oscillators are used by different

¹For a 4×4 LoS MIMO system operating at 10 GHz and with a transmitter and receiver distance of 2 km, the optimal antenna spacing is 3.8 m [12].

users [13]. Thus, the signals at the MIMO receiver may be affected by multiple PHN processes that need to be jointly tracked. Although PHN estimation in MIMO systems has been considered in [6], [14], [15], these approaches do not address the problem of joint PHN estimation and data detection. Consequently, the performances of the schemes in [6], [14], [15] are inferior to the scheme proposed here.

B. Contributions

In this paper, the problem of joint iterative coded PHN estimation and data detection in MIMO systems is addressed. The paper's main contributions are summarized as follows:

- An EM-based receiver for joint PHN estimation and data detection for BICM-MIMO systems is proposed. The EM approach is iteratively applied over the frame, where *low density parity check (LDPC)* codes are used to enhance both data-detection and PHN estimation. To the best of the authors' knowledge, this is the first work that proposes such a receiver structure for tracking nondeterministic parameters, e.g., PHN, over a transmission frame for MIMO systems.
- Unlike the results in [10], it is analytically shown that at high signal-to-noise ratios (SNRs), a maximum a posteriori (MAP) estimator can be used to carry out the maximization step of the EM algorithm. To reduce the computational complexity of the proposed iterative receiver, instead of a MAP estimator, an *extended Kalman filter-smoother (EKFS)* is applied.
- Extensive simulations are carried out for different PHN variances to show that the performance of a MIMO system employing the proposed receiver structure is very close to the ideal case of perfect synchronization. These simulations also demonstrate that the proposed joint estimation and detection approach is far superior to schemes that perform estimation and detection separately, e.g., [15].

C. Organization

The remainder of the paper is organized as follows: Section II presents the system model while the proposed EM-based PHN estimator is derived in Section III. Section IV presents the structure of the iterative detector. Section V presents the complexity analysis for the proposed receiver structure. Finally, Section VI presents the results of our extensive simulations.

D. Notations

Superscripts $(\cdot)^H$ and $(\cdot)^T$ denote the conjugate transpose and transpose operators, respectively. Bold face small letters, e.g., \mathbf{x} , are used for vectors and bold face capital letters, e.g., \mathbf{X} , are used for matrices.

$\mathbf{I}_{X \times X}$ and $\mathbf{0}_{X \times X}$ denote the $X \times X$ identity and all zero matrices, respectively. $\text{diag}(\mathbf{x})$ denotes a diagonal matrix, where the diagonal elements are given by the vector \mathbf{x} . $\|\cdot\|$, $\text{tr}(\cdot)$, $\mathbb{E}\{\cdot\}$, $\Re\{\cdot\}$, and $\Im\{\cdot\}$ denote the Frobenius norm, trace, expectation, real, and imaginary operators, respectively. $p(x|y)$ denotes the probability distribution function of x given y . Finally, $\mathcal{N}(\mu, \sigma^2)$ and $\mathcal{CN}(\mu, \sigma^2)$ denote real and complex Gaussian distributions, respectively, with mean μ and variance σ^2 .

II. SYSTEM MODEL

A MIMO system with N_t transmit antennas and N_r receive antennas is considered. At the transmitter, the coded bits are interleaved and modulated onto an M -point quadrature amplitude modulation (M -QAM) constellation denoted by Ω . Subsequently, using spatial multiplexing, the symbols are transmitted simultaneously from N_t antennas. Frame based transmission is considered, where L_f denotes the frame length. In this paper, the following set of assumptions is adopted:

- A1. Quasi-static block fading channels are considered.
- A2. Training sequences transmitted at the beginning of each frame are used to estimate the channel parameters using the algorithm in [6]. Thus, the subsequent analysis is based on the assumption that the MIMO channel matrix \mathbf{H} is known. However, in Section VI, extensive simulations are carried out by estimating the channel parameters using the algorithm in [6]. The assumption of known channel parameters is justified since the topic of joint channel and PHN estimation using a *known training sequence* is addressed in [6].
- A3. To ensure generality and also applicability of the proposed scheme to LoS and multi-user MIMO systems, it is assumed that independent oscillators are deployed at each transmit and receive antenna.
- A4. PHN is modeled as a discrete-time Wiener process, i.e., PHN at time k , $\theta(k)$ is given by

$$\theta(k) = \theta(k-1) + \Delta(k),$$

where $\Delta(k)$ is the PHN innovation [16].

Assumptions A1 and A3 are in line with previous PHN estimation algorithms in MIMO systems [6], [14], [15]. Moreover, both assumptions are justifiable in many practical scenarios, e.g., in MIMO microwave backhaul links [4], where the channel parameters change much more slowly than the PHN process and independent oscillators are used at each antenna due to the large antenna spacing (2-4 meters).

The received signal vector at time instant k , $\mathbf{y}(k) \triangleq [y_1(k), y_2(k), \dots, y_{N_r}(k)]^T$, is given by

$$\mathbf{y}(k) = \mathbf{\Gamma}^{[r]}(k) \mathbf{H} \mathbf{\Gamma}^{[t]}(k) \mathbf{s}(k) + \mathbf{w}(k), \quad (1)$$

where

- $\mathbf{\Gamma}^{[r]}(k) \triangleq \text{diag}(e^{j\theta_1^{[r]}(k)}, \dots, e^{j\theta_{N_r}^{[r]}(k)})$ and $\mathbf{\Gamma}^{[t]}(k) \triangleq \text{diag}(e^{j\theta_1^{[t]}(k)}, \dots, e^{j\theta_{N_t}^{[t]}(k)})$ are $N_r \times N_r$ and $N_t \times N_t$ diagonal matrices, respectively,
- $\theta_\ell^{[r]}(k)$ and $\theta_m^{[t]}(k)$ denote the PHN process at the ℓ th receive and m th transmit antennas, respectively,
- $\mathbf{H} \triangleq [\mathbf{h}_1, \dots, \mathbf{h}_{N_t}]$ with $\mathbf{h}_\ell \triangleq [h_{\ell,1}, \dots, h_{\ell,N_r}]^T$ is the $N_r \times N_t$ MIMO channel matrix,
- $h_{\ell,m}$, for $\ell = 1, \dots, N_r$ and $m = 1, \dots, N_t$, denotes the channel parameter for the m th receive and ℓ th transmit antennas pair that is assumed to be distributed as $h_{\ell,m} \sim \mathcal{CN}(\mu_{h_{\ell,m}}, \sigma_{h_{\ell,m}}^2)$,
- $\mathbf{s}(k) \triangleq [s_1(k), \dots, s_{N_t}(k)]^T$ is the vector of transmitted symbols,
- $\mathbf{w}(k) \triangleq [w_1(k), \dots, w_{N_r}(k)]^T$ is the vector of the zero-mean additive white Gaussian noise (AWGN) at the receiver, i.e., $w_m \sim \mathcal{CN}(0, \sigma_{w_m}^2)$.

III. THE PROPOSED EM-BASED PHN ESTIMATOR

The EM algorithm consists of the *expectation step (E-step)* and the *maximization step (M-step)* [7] that for the i th EM iteration are given by

$$Q\left(\Theta | \hat{\Theta}^{(i-1)}\right) = \mathbb{E}_{\mathbf{S} | \mathbf{Y}, \hat{\Theta}^{(i-1)}} \left\{ \ln p(\mathbf{Y} | \mathbf{S}, \Theta) \right\} + \ln p(\Theta), \quad (2)$$

$$\hat{\Theta}^{(i)} = \arg \max_{\Theta} \left\{ Q\left(\Theta | \hat{\Theta}^{(i-1)}\right) \right\}, \quad (3)$$

respectively. In (2) and (3), $[\mathbf{Y}]_{N_r \times L_f} \triangleq [\mathbf{y}(1), \mathbf{y}(2), \dots, \mathbf{y}(L_f)]$ and $[\Theta]_{(N_r + N_t) \times L_f} \triangleq [\boldsymbol{\theta}(1), \boldsymbol{\theta}(2), \dots, \boldsymbol{\theta}(L_f)]$. Moreover, since the convergence of the EM algorithm is highly dependent on the initialization process, we propose to transmit pilot symbols every p_r symbol within each transmission frame. In the subsequent subsections, the E- and M-steps of the EM algorithm for coded MIMO systems are derived.

A. E-step

The MIMO received signal vector $\mathbf{y}(k)$ in (1) can be rewritten as

$$\mathbf{y}(k) = \mathbf{X}(k) \mathbf{s}(k) + \mathbf{w}(k), \quad (4)$$

where $\mathbf{X}(k) \triangleq \mathbf{\Gamma}^{[r]}(k)\mathbf{H}\mathbf{\Gamma}^{[t]}(k)$. Accordingly, using straightforward algebraic manipulations, the log likelihood function (LLF) of the received signal matrix, \mathbf{Y} , given the transmitted data, \mathbf{S} , and the PHN process, Θ , can be determined to be proportional to

$$\begin{aligned} \ln p(\mathbf{Y}|\mathbf{S}, \Theta) &\propto - \sum_{k=1}^{L_f} \|\mathbf{y}(k) - \mathbf{X}(k)\mathbf{s}(k)\|^2 \\ &\propto 2\Re \left\{ \sum_{k=1}^{L_f} \text{tr}(\mathbf{y}(k)\mathbf{s}^H(k)\mathbf{X}^H(k)) \right\} - \sum_{k=1}^{L_f} \text{tr}(\mathbf{X}(k)\mathbf{s}(k)\mathbf{s}^H(k)\mathbf{X}^H(k)). \end{aligned} \quad (5)$$

Using (5), the E-step in (2) can be rewritten as

$$Q(\Theta|\hat{\Theta}^{(i-1)}) \propto 2\Re \left\{ \sum_{k=1}^{L_f} \text{tr}(\mathbf{y}(k)\boldsymbol{\alpha}^H(k)\mathbf{X}^H(k)) \right\} - \sum_{k=1}^{L_f} \text{tr}(\mathbf{X}(k)\mathbf{B}(k)\mathbf{X}^H(k)) + \ln p(\Theta), \quad (6)$$

where

$$\boldsymbol{\alpha}(k) \triangleq \sum_{\mathbf{a}_n \in M^{N_t}} \mathbf{a}_n p(\mathbf{s}(k) = \mathbf{a}_n | \mathbf{Y}, \hat{\Theta}^{(i-1)}) \quad (7)$$

$$\mathbf{B}(k) \triangleq \sum_{\mathbf{a}_n \in M^{N_t}} \mathbf{a}_n \mathbf{a}_n^H p(\mathbf{s}(k) = \mathbf{a}_n | \mathbf{Y}, \hat{\Theta}^{(i-1)}). \quad (8)$$

Here, $\boldsymbol{\alpha}(k)$ denotes the marginal posterior mean of the coded symbol vector at time k , i.e., the soft decisions, and $p(\mathbf{s}(k) = \mathbf{a}_n | \mathbf{Y}, \hat{\Theta}^{(i-1)})$ denotes the a posteriori probabilities (APPs) of the coded symbol vector given \mathbf{Y} and $\hat{\Theta}^{(i-1)}$. Note that at high SNR, i.e., $p(\mathbf{s}(k) = \mathbf{a}_n | \mathbf{Y}, \hat{\Theta}^{(i-1)}) = 0, \forall k \neq n$, $\boldsymbol{\alpha}(k) = \mathbf{s}(k)$ and $\mathbf{B}(k) = \mathbf{s}(k)\mathbf{s}^H(k)$.

B. M-step

In this section, we seek to show that a MAP estimator can be applied to carry out the M-step of the proposed EM-based PHN estimator at high SNR. Given the observation matrix \mathbf{Y} , the MAP estimate of $\hat{\Theta}$ is given by [17]

$$\hat{\Theta} = \arg \max_{\Theta} \{ \ln p(\mathbf{Y}|\Theta, \mathbf{S} = \mathbf{A}) + \ln p(\mathbf{S} = \mathbf{A}) + \ln p(\Theta) \}, \quad (9)$$

where $[\mathbf{A}]_{N_t \times L_f} \triangleq [\boldsymbol{\alpha}(1), \boldsymbol{\alpha}(2), \dots, \boldsymbol{\alpha}(L_f)]$. Assuming equally probable transmitted symbols, at high SNR, i.e., $p(\mathbf{s}(k) = \mathbf{a}_n | \mathbf{Y}, \hat{\Theta}^{(i-1)}) = 0, \forall k \neq n$, (9) can be rewritten as

$$\hat{\Theta} = \arg \max_{\Theta} \{ \ln p(\mathbf{Y}|\Theta, \mathbf{S} = \mathbf{A}) + \ln p(\Theta) \} \quad (10a)$$

$$= \arg \max_{\Theta} \left\{ 2\Re \left\{ \sum_{k=1}^{L_f} \text{tr}(\mathbf{y}(k)\mathbf{s}^H(k)\mathbf{X}^H(k)) \right\} - \sum_{k=1}^{L_f} \text{tr}(\mathbf{X}(k)\mathbf{s}(k)\mathbf{s}^H(k)\mathbf{X}^H(k)) + \ln p(\Theta) \right\}. \quad (10b)$$

Based on the discussion following (6), the results in (6) and (10b) are equivalent at high SNR. Thus, (10b) is in fact maximizing the E-Step in (6), which indicates that a MAP estimator can be applied to carry out the M-step of the proposed EM algorithm at high SNR.

It is important to indicate that although a MAP estimator can be applied to carry out the M-step of the EM algorithm, solving for the MAP solution in (10b) requires a multidimensional exhaustive search that is computationally very intensive. Thus, we propose to apply a Kalman filter, which is an optimal linear minimum mean square error estimator [17], to carry out the maximization step of the EM algorithm and reduce its computational complexity. The set of EKFS equations are provided in following subsection.

C. The Extended Kalman Filter-Smoother

In this subsection a low complexity EKFS is applied to carry out the M-step of the EM algorithm. We first note that due to a phase ambiguity, the $N_r + N_t$ PHN parameters $\boldsymbol{\theta}(k)$ cannot be jointly estimated [14]. Instead, by arbitrarily selecting the PHN process, $\theta_{N_t}^{[t]}(k)$, as a reference PHN value, $\mathbf{X}(k)$ in (4) can be rewritten as [15]

$$\mathbf{X}(k) = \tilde{\mathbf{\Gamma}}^{[r]}(k) \mathbf{H} \tilde{\mathbf{\Gamma}}^{[t]}(k), \quad (11)$$

where $\tilde{\mathbf{\Gamma}}^{[r]}(k) \triangleq \text{diag}\{e^{j(\phi_1(k))}, \dots, e^{j(\phi_{N_r}(k))}\}$, $\tilde{\mathbf{\Gamma}}^{[t]}(k) \triangleq \text{diag}\{e^{j(\phi_{N_r+1}(k))}, \dots, e^{j(\phi_{N_r+N_t-1}(k))}, 1\}$, $\boldsymbol{\phi}(k) \triangleq [\phi_1(k), \dots, \phi_{N_r+N_t-1}(k)]^T$, and

$$\phi_f(k) \triangleq \begin{cases} \theta_f^{[r]} + \theta_{N_t}^{[t]} & f = 1, \dots, N_r, \\ \theta_{f-N_r}^{[t]} - \theta_{N_t}^{[t]} & f = N_r + 1, \dots, N_r + N_t - 1. \end{cases}$$

The application of the equivalent signal model in (11) instead of (1) eliminates the ambiguity associated with the estimation of PHN parameters. Subsequently, the state and observation equations can be determined as

$$\boldsymbol{\phi}(k) = \boldsymbol{\phi}(k-1) + \tilde{\boldsymbol{\Delta}}(k), \quad (12)$$

$$\mathbf{y}(k) \approx \mathbf{z}(\boldsymbol{\phi}(k)) + \mathbf{w}(k), \quad (13)$$

where $\mathbf{z}(\boldsymbol{\phi}(k)) \triangleq [z_1(\boldsymbol{\phi}(k)), z_2(\boldsymbol{\phi}(k)), \dots, z_{N_r}(\boldsymbol{\phi}(k))]^T = \tilde{\mathbf{\Gamma}}^{[r]}(k) \mathbf{H} \tilde{\mathbf{\Gamma}}^{[t]}(k) \boldsymbol{\alpha}(k)$, $\tilde{\boldsymbol{\Delta}}(k) \triangleq [\Delta_1^{[r]}(k) + \Delta_{N_t}^{[t]}(k), \dots, \Delta_{N_r}^{[r]}(k) + \Delta_{N_t}^{[t]}(k), \Delta_1^{[t]}(k) - \Delta_{N_t}^{[t]}(k), \dots, \Delta_{N_t-1}^{[t]}(k) - \Delta_{N_t}^{[t]}(k)]^T$, and $\Delta_\ell^{[r]}(k)$ and $\Delta_m^{[t]}(k)$ are the PHN innovations corresponding to the ℓ th receive and m th transmit antenna PHN parameters,

$\theta_\ell^{[r]}(k)$ and $\theta_m^{[t]}(k)$, respectively [18]. $\Delta_\ell^{[r]}(k)$ and $\Delta_m^{[t]}(k)$, $\forall \ell, m$, are modelled as real Gaussian processes, i.e., $\Delta_\ell^{[r]}(k), \Delta_m^{[t]}(k) \sim \mathcal{N}(0, \sigma_\Delta^2)$, $\forall \ell, m$ [6], [18]. Moreover, $\alpha(k)$ is defined after (6). Note that since $z_m(\phi(k))$ is a nonlinear function of $\phi(k)$ the extended Kalman filter is applied here.

Recall that *complex* channel parameters (consisting of the channel gain and *phase*) are estimated at the start of the frame via a training sequence and the algorithm in [6]. Consequently, the EKFS is initialized with the state estimate $\hat{\phi}(0) = \mathbf{0}_{(N_t+N_r-1) \times 1}$ and the error covariance matrix $\hat{\mathbf{M}}(0) = 2\sigma_\Delta^2 \mathbf{I}$. Subsequently, the EKFS determines the a priori state vector, $\hat{\phi}^-(k)$, and the a priori error covariance matrix, $\left[\hat{\mathbf{M}}^-(k)\right]_{(N_r+N_t-1) \times (N_r+N_t-1)}$, using $\hat{\phi}^-(k) = \hat{\phi}^-(k-1)$ and $\hat{\mathbf{M}}^-(k) = \hat{\mathbf{M}}^-(k-1) + 2\sigma_\Delta^2 \mathbf{I}$, respectively. The EKFS linearizes the nonlinear function $\mathbf{z}(\phi(k))$ in (13) about the a priori estimate of the state vector via

$$\mathbf{z}(\phi(k)) \approx \mathbf{z}(\hat{\phi}^-(k)) + \dot{\mathbf{Z}}(k)(\phi(k) - \hat{\phi}^-(k)), \quad (14)$$

where the Jacobian matrix with respect to ϕ at time instance k , $\left[\dot{\mathbf{Z}}(k)\right]_{N_r \times (N_r+N_t-1)}$, can be determined as

$$\dot{\mathbf{Z}}(k) \triangleq \left. \frac{\partial \mathbf{z}}{\partial \phi(k)} \right|_{\hat{\phi}^-(k)} = \left[\dot{\mathbf{Z}}_1(k), \dot{\mathbf{Z}}_2(k) \right]. \quad (15)$$

In (15), the matrix $\left[\dot{\mathbf{Z}}_1(k)\right]_{N_r \times N_r}$ is given by

$$\dot{\mathbf{Z}}_1(k) \triangleq \text{diag} \left\{ j z_1(\hat{\phi}^-(k)), \dots, j z_{N_r}(\hat{\phi}^-(k)) \right\}, \quad (16)$$

and the matrix $\left[\dot{\mathbf{Z}}_2(k)\right]_{N_r \times (N_t-1)}$ is determined as

$$\dot{\mathbf{Z}}_2(k) \triangleq \begin{bmatrix} j h_{11} e^{j \hat{\phi}_1^-(k)} \alpha_1(k) e^{j \hat{\phi}_{N_r+1}^-(k)} & \dots & j h_{1(N_t-1)} e^{j \hat{\phi}_1^-(k)} \alpha_{N_t-1}(k) e^{j \hat{\phi}_{N_r+N_t-1}^-(k)} \\ j h_{21} e^{j \hat{\phi}_2^-(k)} \alpha_1(k) e^{j \hat{\phi}_{N_r+1}^-(k)} & \dots & j h_{2(N_t-1)} e^{j \hat{\phi}_2^-(k)} \alpha_{N_t-1}(k) e^{j \hat{\phi}_{N_r+N_t-1}^-(k)} \\ \vdots & \ddots & \vdots \\ j h_{N_r 1} e^{j \hat{\phi}_{N_r}^-(k)} \alpha_1(k) e^{j \hat{\phi}_{N_r+1}^-(k)} & \dots & j h_{N_r(N_t-1)} e^{j \hat{\phi}_{N_r}^-(k)} \alpha_{N_t-1}(k) e^{j \hat{\phi}_{N_r+N_t-1}^-(k)} \end{bmatrix}. \quad (17)$$

After the observation, the posteriori estimate of the state vector, denoted by $\hat{\phi}^+(k)$, and the posteriori error covariance matrix, denoted by $\hat{\mathbf{M}}^+(k)$, are determined as

$$\hat{\phi}^+(k) = \hat{\phi}^-(k) + \Re \{ \mathbf{K}(k) (\mathbf{y}(k) - \mathbf{z}(\hat{\phi}^-(k))) \}, \quad (18a)$$

$$\hat{\mathbf{M}}^+(k) = \left(\mathbf{I} - \Re \{ \mathbf{K}(k) \dot{\mathbf{Z}}(k) \} \right) \hat{\mathbf{M}}^-(k), \quad (18b)$$

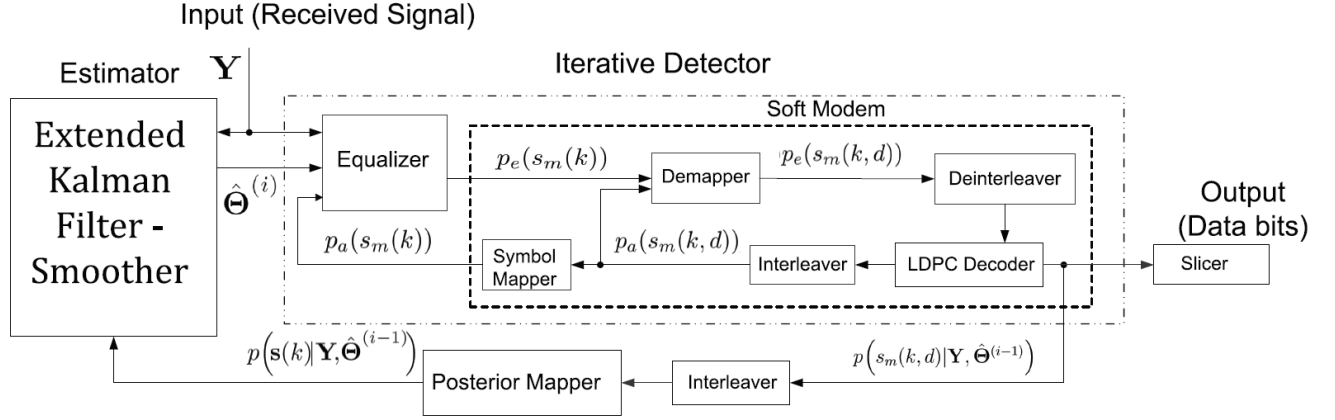


Fig. 1. Block diagram of the receiver structure, where d denotes the number of iterations within the soft-modem.

where $\mathbf{K}(k) = \hat{\mathbf{M}}^-(k) \dot{\mathbf{Z}}(k)^H (\mathbf{C}_w + \dot{\mathbf{Z}}(k) \hat{\mathbf{M}}^-(k) \dot{\mathbf{Z}}(k)^H)^{-1}$ is the $(N_r + N_t - 1) \times N_r$ Kalman Gain matrix and $\mathbf{C}_w = \left(\frac{\sigma_w^2}{2} + j\frac{\sigma_w^2}{2}\right) \mathbf{I}$ is the observation noise covariance matrix. The EKFS also runs a backward recursion to smooth the a posteriori estimates of the state statistics over the block. The smoothed estimate of the PHN vector, $\hat{\phi}(k)$, and the error covariance matrix $\hat{\mathbf{M}}(k)$ are given by

$$\hat{\phi}(k) = \hat{\phi}^+(k) + \hat{\mathbf{M}}^+(k) (\hat{\mathbf{M}}^-(k+1))^{-1} (\hat{\phi}(k+1) - \hat{\phi}^-(k+1)) \quad (19a)$$

$$\hat{\mathbf{M}}(k) = \hat{\mathbf{M}}^+(k) + \hat{\mathbf{M}}^+(k) (\hat{\mathbf{M}}^-(k+1))^{-1} (\hat{\mathbf{M}}(k+1) - \hat{\mathbf{M}}^-(k+1)) (\hat{\mathbf{M}}^+(k) (\hat{\mathbf{M}}^-(k+1))^{-1})^T. \quad (19b)$$

After the backward recursion is completed, the block of PHN estimates, $\hat{\phi}(k)$, for $k = 1, 2, \dots, L_f$, are fed to the iterative detector, which is presented in the following section.

IV. ITERATIVE DETECTOR

As indicated in Sec. III-B, the soft decisions, \mathbf{A} , are required by the EKFS to estimate the PHN parameters. However, the computation of the true posterior probabilities has a complexity that increases exponentially with the frame length L_f . Therefore, here, a near optimal iterative detector is used in combination with a soft modulator to map the a posteriori bit probabilities to symbol probabilities and construct the soft decisions [3],[19],[11]. The block diagram of the proposed EM-based receiver structure, including both the EKFS and the iterative detector, is shown in Fig. 1. Note that since an interleaver at the transmitter side is used, the symbols transmitted from each antenna and the bits within each symbol are independent.

In order to describe the structure of the proposed iterative detector, we introduce the following notations:

- $p(\cdot)$, $p_a(\cdot)$, and $p_e(\cdot)$ denote *a posteriori*, *a priori*, and *extrinsic* probabilities, respectively.
- $p\left(s_m(k)|\mathbf{Y}, \hat{\Theta}^{(i-1)}\right)$ is the conditional *a posteriori* probability of the transmitted symbol at the transmit antenna m , at time instance k , $s_m(k)$. According to the turbo principle, it can be factored as

$$p\left(s_m(k)|\mathbf{Y}, \hat{\Theta}^{(i-1)}\right) = C^{(1)}p_a(s_m(k))p_e(s_m(k)). \quad (20)$$

where $p_a(s_m(k))$ is the a priori symbol probability, $p_e(s_m(k))$ is the extrinsic symbol probability, and $C^{(1)}$ is a normalization constant. The conditional terms in the extrinsic and the a priori probabilities are omitted for notational simplicity. Note that, these posterior probabilities are used to construct the soft decision, $\alpha(k)$, which is required by the M-step.

- Similarly, $p\left(s_m(k, d)|\mathbf{Y}, \hat{\Theta}^{(i-1)}\right)$ denotes the *bit posterior probabilities* of the d th bit of the bit sequence mapped to the symbol $s_m(k)$, denoted as $s_m(k, d)$. $p\left(s_m(k, d)|\mathbf{Y}, \hat{\Theta}^{(i-1)}\right)$ is given as a product of the a priori bit probabilities, $p_a(s_m(k, d))$, the extrinsic bit probabilities $p_e(s_m(k, d))$, and a normalization constant, $C^{(2)}$. Note that the posterior bit probabilities, $p\left(s_m(k, d)|\mathbf{Y}, \hat{\Theta}^{(i-1)}\right)$, are used for hard decision at the end of a number of EM iterations.
- $p\left(\mathbf{Y}|\mathbf{s}(k), \hat{\Theta}^{(i-1)}\right)$ denotes the conditional likelihoods of the symbol vectors computed by the equalizer from the received signal before the execution of the detector iterations.

The proposed iterative receiver computes the symbol and bit probabilities according to in Algorithm 1 on the next page and by utilizing the following set of equations:

Equalizer:

$$\begin{aligned} p\left(\mathbf{Y}|\mathbf{s}(k), \hat{\Theta}^{(i-1)}\right) &= p\left(\mathbf{y}(k)|\mathbf{s}(k), \hat{\Theta}^{(i-1)}\right) \\ &= C^{(3)} \exp\left(-\frac{1}{2\sigma_w^2}|\mathbf{y}(k) - \mathbf{X}(k)\mathbf{s}(k)|^2\right), \end{aligned} \quad (21)$$

$$\begin{aligned} p_e(s_m(k) = a_n) &= p\left(\mathbf{Y}|s_m(k) = a_n, \hat{\Theta}^{(i-1)}\right) \\ &= \sum_{\mathbf{s}(k):s_m(k)=a_n} \left\{ p\left(\mathbf{Y}|\mathbf{s}(k), \hat{\Theta}^{(i-1)}\right) \prod_{m' \neq m} p_a(s_{m'}(k)) \right\}, \end{aligned} \quad (22)$$

Algorithm 1: The Iterative Detector Algorithm for the E-step at the i -th EM iteration

input : $\hat{\Theta}^{(i-1)}, \mathbf{H}$
output: $\alpha(k), \hat{s}_m(k, d), \quad \forall k, m, d$
 1 $p(\mathbf{Y}|\mathbf{s}(k), \hat{\Theta}^{(i-1)}) \leftarrow (21), \quad \forall k$
 2 **for** $l := 1$ **to** L_{eq-sm} **do**
 3 $p_e(s_m(k)) \leftarrow (22), \quad \forall k, m$
 4 **for** $b := 1$ **to** L_{dm-dc} **do**
 5 $p_e(s_m(k, d)) \leftarrow (23), \quad \forall k, m, d$
 6 Deinterleave
 7 $p_a(s_m(k, d)) \leftarrow$ LDPC decoder
 8 $p(s_m(k, d)|\mathbf{Y}, \hat{\Theta}^{(i-1)}) \leftarrow$ LDPC decoder
 9 Interleave
 10 **end**
 11 $p_a(s_m(k)) \leftarrow (24), \quad \forall k, m$
 12 **end**
 13 $p(\mathbf{s}(k)|\mathbf{Y}, \hat{\Theta}^{(i-1)}) \leftarrow (26), \quad \forall k$
 14 $\alpha(k) \leftarrow p(\mathbf{s}(k)|\mathbf{Y}, \hat{\Theta}^{(i-1)}), \quad \forall k$
 15 $\hat{s}_m(k, d) \leftarrow p(s_m(k, d)|\mathbf{Y}, \hat{\Theta}^{(i-1)}), \quad \forall k$

Demapper:

$$\begin{aligned}
 p_e(s_m(k, d) = \beta) &= p(\mathbf{Y}|s_m(k, d) = \beta, \hat{\Theta}^{(i-1)}) \\
 &= \sum_{a_n \in \Omega: a_n(d) = \beta} \left\{ p_e(s_m(k) = a_n) \prod_{d' \neq d} p_a(s_m(k, d')) \right\}, \tag{23}
 \end{aligned}$$

Symbol mapper:

$$p_a(s_m(k)) = \prod_d p_a(s_m(k, d)), \tag{24}$$

Posterior mapper:

$$p(\mathbf{s}(k)|\mathbf{Y}, \hat{\Theta}^{(i-1)}) = C^{(4)} p_a(\mathbf{s}(k)) p_e(\mathbf{s}(k)) \quad (25)$$

$$= C^{(5)} p(\mathbf{Y}|\mathbf{s}(k), \hat{\Theta}^{(i-1)}) \prod_{m,d} p_a(s_m(k, d)) \quad (26)$$

where $a_n \in \Omega, n = 1, 2, \dots, M, \beta \in \{0, 1\}$, and $C^{(3)}, C^{(4)}$, and $C^{(5)}$ are normalization constants. In Algorithm 1, L_{eq-sm} is the number of iterations between the *equalizer* and the *soft modem* and L_{dm-dc} is the number of iterations between the *demapper* and *LDPC decoder*.

The a priori symbol probabilities, $p_a(s_m(k))$, and bit probabilities, $p_a(s_m(k, d))$, are initialized with a uniform distribution at the first EM algorithm iteration. Subsequently, the detector is initialized with the a priori probabilities obtained at the previous EM iteration.

V. COMPLEXITY ANALYSIS

In this paper, computational complexity is defined as the number of complex additions plus multiplications required to obtain the PHN estimates at the i -th iteration, $\hat{\Theta}^{(i)}$. Throughout this subsection, the superscripts $(\cdot)^{[M]}$ and $(\cdot)^{[A]}$ are used to denote the number of multiplications and additions required by each algorithm, respectively. In order to reduce the computational complexity of the MAP estimator, it is assumed that alternating projection is applied to carry out the multidimensional exhaustive search in (10b) [20]. Subsequently, the complexity of the MAP estimator in (10b), denoted by $C_{MAP} \triangleq C_{MAP}^{[M]} + C_{MAP}^{[A]}$, can be determined as

$$C_{MAP}^{[M]} = \mathcal{N}(N_r + N_t) L_f \frac{2\pi}{\kappa} \left\{ 1 + L_f \left(\underbrace{N_r N_t + N_r^2 N_t}_{\text{first factor in (10b)}} + \underbrace{2N_r N_t + N_r^2 N_t}_{\text{second factor in (10b)}} + \underbrace{N_r^2 N_t + N_r N_t^2}_{\mathbf{x}(k) \text{ in (10b)}} + C_{\alpha(k)}^{[M]} \right) \right\}, \quad (27)$$

$$C_{MAP}^{[A]} = \mathcal{N}(N_r + N_t) L_f \frac{2\pi}{\kappa} \left\{ 2 + L_f \left(\underbrace{N_r^2 (N_t - 1) + N_r}_{\text{first factor in (10b)}} + \underbrace{N_r^2 (N_t - 1) + N_r N_t}_{\text{second factor in (10b)}} \right. \right. \\ \left. \left. + \underbrace{N_r N_t (N_r + N_t - 2)}_{\mathbf{x}(k) \text{ in (10b)}} + C_{\alpha(k)}^{[A]} \right) \right\}, \quad (28)$$

where

$$\begin{aligned}
C_{\alpha^{(k)}}^{[M]} &= \underbrace{N_t M^{N_t}}_{(7)} + M^{N_t} \left\{ \underbrace{N_r N_t + N_r + 3}_{(21)} + \underbrace{N_t \log_2 M + 2}_{(26)} + L_{eq-sm} \left[\underbrace{N_t M^{N_t-1}}_{(22)} + \underbrace{N_t}_{(24)} \right. \right. \\
&\quad \left. \left. + L_{dm-dc} \left(\underbrace{\frac{M}{2} \log_2 M}_{(23)} + \underbrace{L_{dec} N_{var}}_{\text{LDPC decoder}} \right) \right] \right\},
\end{aligned}$$

$$\begin{aligned}
C_{\alpha^{(k)}}^{[A]} &= \underbrace{N_t (M^{N_t} - 1)}_{(7)} + M^{N_t} \left\{ \underbrace{N_r N_t + N_r - 1}_{(21)} + L_{eq-sm} \left[\underbrace{M^{N_t-1} - 1}_{(22)} \right. \right. \\
&\quad \left. \left. + L_{dm-dc} \left(\underbrace{\frac{M}{2} - 1}_{(23)} + \underbrace{L_{dec} (2N_{check} - 1)}_{\text{LDPC decoder}} \right) \right] \right\},
\end{aligned}$$

- \mathcal{N} denotes the number of alternating projection cycles used,
- κ denotes the step size used for the exhaustive search,
- L_{eq-sm} is the number of iterations between the equalizer and the soft modem,
- L_{dm-dc} is the number of iterations between the demapper and LDPC decoder, and
- N_{var} and N_{check} denote the number of variable nodes and check nodes of the regular LDPC code, respectively.

The complexity of the proposed EKFS, $C_{EKFS} = C_{EKFS}^{[M]} + C_{EKFS}^{[A]}$, can be calculated as

$$\begin{aligned}
C_{EKFS}^{[M]} &= L_f \left\{ \underbrace{2N^2 N_r + 2N_r^2 N + N_r^3}_{\mathbf{K}(k) \text{ below (18b)}} + \underbrace{N_r + 5N_r(N_t - 1)}_{\dot{\mathbf{z}}(k) \text{ in (15)}} + \underbrace{N(N_r + 1)}_{(18a)} + \underbrace{N(NN_r + N^2 + 1)}_{(18b)} \right. \\
&\quad \left. + \underbrace{N_r^2 N_t + N_r N_t^2 + N_r N_t}_{\mathbf{z}(\hat{\phi}^-(k)) \text{ in (18a)}} + C_{\alpha^{(k)}}^{[M]} + \underbrace{N^2 + N^3}_{(19a)} + \underbrace{2N^3}_{(19b)} \right\}, \quad (29)
\end{aligned}$$

$$\begin{aligned}
C_{EKFS}^{[A]} &= L_f \left\{ \underbrace{N}_{(12)} + \underbrace{NN_r(2N + N_r - 3) + N_r^2 N + N_r^3}_{\mathbf{K}(k) \text{ below (18b)}} + \underbrace{N_r(N + 1)}_{(18a)} + \underbrace{N^2(N + N_r - 1)}_{(18b)} \right. \\
&\quad \left. + \underbrace{N_r N_t(N_r + N_t - 1) - N_r}_{\mathbf{z}(\hat{\phi}^-(k)) \text{ in (18a)}} + C_{\alpha^{(k)}}^{[A]} + \underbrace{N(N^2 + 1)}_{(19a)} + \underbrace{N^2(2N + 1)}_{(19b)} \right\}, \quad (30)
\end{aligned}$$

where $N \triangleq N_r + N_t - 1$.

Remark 1: In Table I, the computational complexity of the MAP and EKFS estimators are compared against one another for 2×2 , 4×4 , and 8×8 MIMO systems. To ensure accurate estimation via the MAP estimator, we set $\kappa = 10^{-3}$ and $\mathcal{N} = 4$. It is also assumed that a rate $R = 7/8$ regular LDPC

TABLE I

COMPUTATIONAL COMPLEXITY OF THE MAP AND EKFS ESTIMATORS FOR DIFFERENT NUMBER OF ANTENNAS.

MIMO	C_{MAP}	C_{EKFS}
2×2	2.81e17	3.44e8
4×4	7.36e21	4.47e12
8×8	6.20e31	1.89e22

code [21] with a variable node degree of $N_{var} = 4$, check node degree of $N_{check} = 32$, and a frame length of $L_f = 8176$ is used. In addition, $L_{eq-dm} = L_{dm-dc} = L_{dec} = 1$. This approach requires more EM iterations but less detector iterations to converge, which further reduces the computational complexity of the proposed iterative detector significantly. Table I shows that the proposed soft-input EKFS is significantly less computationally complex than the MAP estimator. For example, for a 4×4 MIMO system, the EKFS estimator is 1.6×10^9 times less complex than the MAP estimator.

VI. SIMULATION RESULTS

In this section, the proposed iterative coded receiver structure is extensively simulated. At the transmitter, data bits are first encoded by a rate $R = 7/8$ regular LDPC encoder with variable node degrees of 4 and check node degree of 32 [21]. Gray mapping is applied. The number of data bits in each frame, L_b is set to 7154. In order to enhance bandwidth efficiency, 16-QAM modulation is employed. Performance is measured as a function of E_b/N_0 , where E_b denotes the transmitted power per bit and N_0 is the AWGN power, i.e., $\sigma_w^2 = N_0$. Unless otherwise specified, the number of iterations within the LDPC decoder, L_{dec} , is set to 1. A 2×2 MIMO system is used for all simulations and Rician Fading channels are considered, i.e., $\mu_{h_{m,\ell}} = 0$, $\sigma_{h_{m,\ell}}^2 = 1$, $\forall m, \ell$. The MIMO channel matrix is generated as a sum of LoS and *non-line-of-sight (NLoS)* components, where the Rician factor, ρ , is set to 2 dB throughout this section [12]. The channel parameters are estimated using the approach in [6]. Finally, in the initial step, the EKFS is applied to estimate the PHN parameters corresponding to every p_r spaced pilot. Afterwards, using linear interpolation, the PHN corresponding to the remaining symbols are estimated. These PHN values are then used by the proposed iterative detector to initialize the proposed EM-based algorithm.

In order to thoroughly investigate the performance of the proposed receiver, the following specific simulation scenarios are considered:

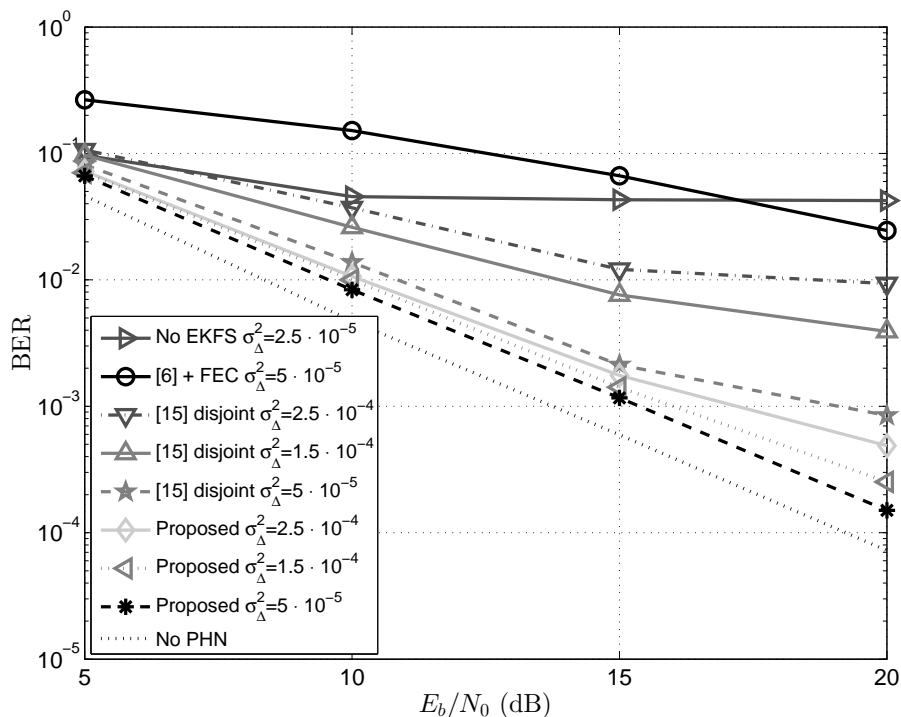


Fig. 2. BER performance of the proposed EM-based algorithm (3 EM iterations with $L_{dec} = 1$).

Scenario 1. The performance of a MIMO receiver that does not track the PHN parameters is simulated. This scenario is denoted by “no PHN tracking”.

Scenario 2. The performance of the proposed iterative receiver is compared to that of [6]. To ensure a fair comparison, the performance of the algorithm in [6] is complemented by FEC, i.e. the above LPDC code is used.² This scenario is denoted by “[6] + FEC”.

Scenario 3. To demonstrate the advantage of the proposed joint PHN estimation and data detection algorithm, the performance of the proposed MIMO receiver is compared to the scenario where PHN estimation and data detection are carried out separately, e.g., the approach in [15]. This scenario is denoted by “[15] disjoint”.

Scenario 4. As a benchmark the performance of a MIMO system that is affected by no PHN is also presented. This scenario is denoted by “No PHN”.

Since the algorithms in [6] and [15] are shown to be superior to the approach in [14], we do not present any comparison results with respect to [14].

In Fig. 2, the bit error-rate (BER) performance of the proposed EM-receiver is investigated. In this

²The results in [6] are presented for uncoded MIMO systems.

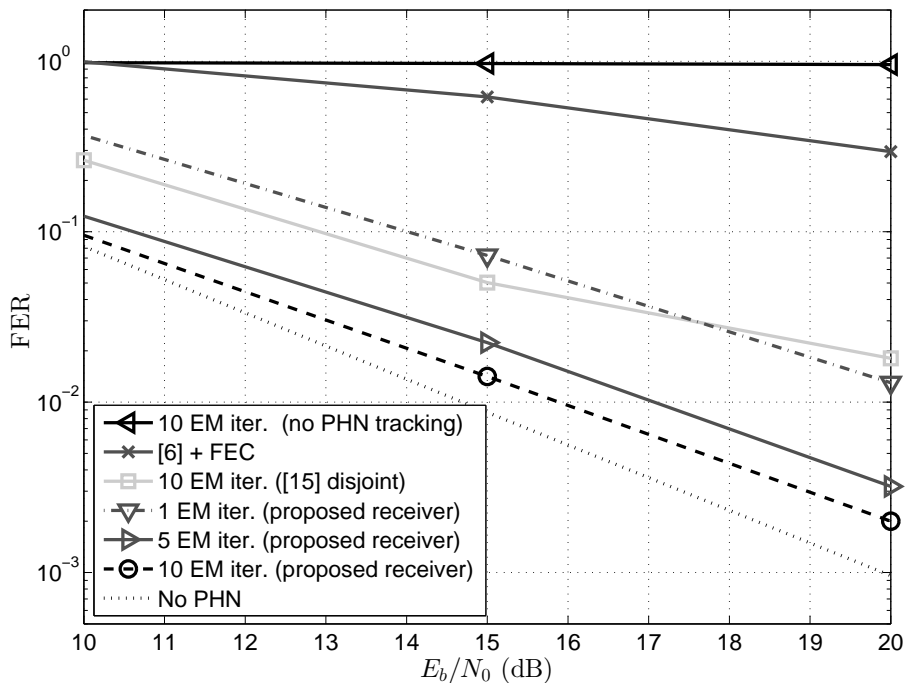


Fig. 3. FER of the proposed EM-based receiver ($\sigma_{\Delta}^2 = 5 \cdot 10^{-5} \text{ rad}^2$).

setup, pilot symbols are transmitted every 14 symbols and only 3-EM iterations are applied at the receiver. Compared to the “no PHN” scenario, the proposed EM-based algorithm gives rise to a BER degradation of about 1.5 dB and 2 dB for PHN variances of $\sigma_{\Delta}^2 = 5 \cdot 10^{-5} \text{ rad}^2$ and $\sigma_{\Delta}^2 = 1.5 \cdot 10^{-4} \text{ rad}^2$, respectively. We also observe that for large PHN variances, i.e., $2.5 \cdot 10^{-4} \text{ rad}^2$, the overall systems suffers from an error floor.³ This follows from the fact that the prediction error of the EKFS is determined by the PHN innovation variance. It is also observed that the performance of a MIMO system is significantly degraded when no PHN tracking is applied. More importantly, the results in Fig. 2 illustrate that by jointly carrying out PHN estimation and data detection, the proposed receiver results in significant performance gains compared to scenario where PHN estimation and data detection are carried out separately, e.g., [15]. In fact, on average, a performance gain of more than 10 dB is observed by applying the proposed receiver.

Fig. 3 shows the frame error-rate (FER) performance of the proposed receiver for a PHN variance of $\sigma_{\Delta}^2 = 5 \cdot 10^{-5} \text{ rad}^2$. It can be seen that the FER performance of the proposed EM receiver improves with each EM iteration. Moreover, as anticipated a MIMO receiver fails to accurately detect the received

³As shown in [18], in practice, the PHN innovation variance is small, e.g., for a typical free-running oscillator operating at 2.8 GHz, the PHN variance is calculated to be $\sigma_{\Delta}^2 = 5 \times 10^{-5} \text{ rad}^2$.

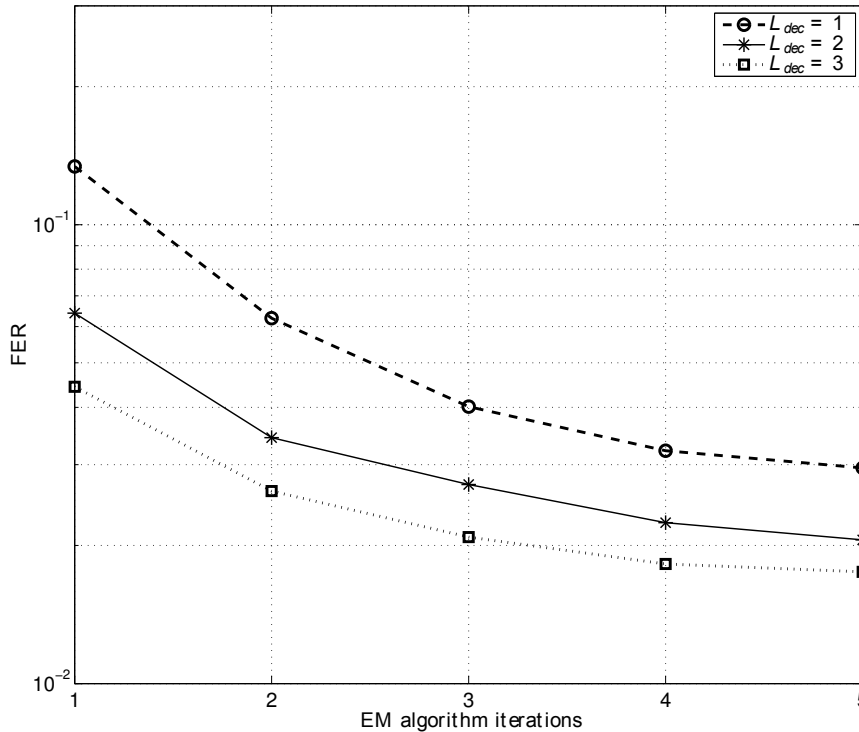


Fig. 4. FER of the proposed EM-based receiver for several number of decoder iterations ($\sigma_{\Delta}^2 = 5 \cdot 10^{-4} \text{ rad}^2$).

signal when no PHN tracking is applied. The results in this figure also corroborate the results in Fig. 2, showing that the proposed joint estimation and detection scheme results in significant performance gains compared to an algorithm that carries out PHN estimation and data detection separately. More specifically, a minimum performance gain of 6 dB is observed for the same number of EM iterations. Moreover, the results in Fig. 3 show that the approach in [6] combined with FEC fails to achieve good frame error performance in low-to-medium SNRs. Finally, it can be observed that in this setup after 10 EM iterations, the FER performance of the proposed receiver is only 2 dB apart from that of perfect synchronization, i.e., “No PHN”.

In Fig. 4 the performance of the proposed EM receiver is investigated for different number of EM and decoder iterations, L_{dec} . In this figure, the SNR is fixed at $E_b/N_0 = 20 \text{ dB}$, while the PHN variance is increased to $\sigma_{\Delta}^2 = 5 \cdot 10^{-4} \text{ rad}^2$. We observe that the performance of the system improves after a few EM iterations. Moreover, the FER performance of the system can be further improved via more iterations inside of the decoder. Thus, the results in Fig. 4 show that the overall performance of the MIMO system

can be enhanced by increasing the number of EM or decoder iterations, which represents a clear trade-off between performance and complexity for system design.

VII. CONCLUSION

In this paper, an iterative EM-based receiver for joint PHN estimation and data detection in MIMO systems is proposed. It is demonstrated that at high SNRs, a MAP estimator can be applied to carry out the maximization step of the EM-based algorithm. However, to reduce the computational complexity of the proposed receiver, instead of a MAP estimator, an EKFS is used to carry out the maximization step of the EM algorithm. Simulation results show that the proposed receiver significantly enhances system performance. In fact, for moderate PHN variances, the overall system performance is only 1.5 dB away from the idealistic case of perfect synchronization while applying a 7/8 rate LDPC code. Simulation results also demonstrate that compared to receiver designs that perform PHN estimation and data detection separately, the proposed receiver results in 10 dB and 6 dB performance gains in terms of BER and FER, respectively. Finally, simulations indicate that the performance of the overall MIMO system can be enhanced in the presence of PHN by increasing the number of EM or decoder iterations.

REFERENCES

- [1] A. O. Isikman, *Phase Noise Estimation for Uncoded/Coded SISO and MIMO Systems*. Master's Thesis, Chalmers University of Technology, Sweden, Oct. 2012. [Online]. Available: <http://arxiv.org/abs/1210.6267>
- [2] I. E. Telatar, "Capacity of multi-antenna Gaussian channels," *European Trans. on Telecommun.*, vol. 10, pp. 585–595, 1999.
- [3] A. Stefanov *et al.*, "Turbo-coded modulation for systems with transmit and receive antenna diversity over block fading channels: system model, decoding approaches, and practical considerations," *IEEE J. Sel. Areas Commun.*, vol. 19, no. 5, pp. 958–968, May 2001.
- [4] J. Wells, *Multi-Gigabit Microwave and Millimeter-Wave Wireless Communications*. First Edition. Artech House, 2010.
- [5] H. Meyr, M. Moeneclaey, and S. A. Fechtel, *Digital Communication Receivers: Synchronization, Channel Estimation, and Signal Processing*. Wiley-InterScience, John Wiley & Sons, Inc., 1997.
- [6] H. Mehrpouyan *et al.*, "Joint estimation of channel and oscillator phase noise in MIMO systems," *IEEE Trans. Signal Process.*, vol. 60, no. 9, pp. 4790–4807, Sep. 2012.
- [7] C. Herzet *et al.*, "Code-aided turbo synchronization," *Proc. IEEE*, vol. 95, no. 6, pp. 1255–1271, Jun. 2007.
- [8] V. Lottici and M. Luise, "Embedding carrier phase recovery into iterative decoding of turbo-coded linear modulations," *IEEE Trans. Commun.*, vol. 52, no. 4, pp. 661–669, Apr. 2004.
- [9] N. Noels, *et al.*, "A theoretical framework for soft-information-based synchronization in iterative (turbo) receivers," *EURASIP Wireless Communication Networks*, no. 2, pp. 117–129, 2005.
- [10] T. Shehata and M. El-Tanany, "Joint iterative detection and phase noise estimation algorithms using kalman filtering," in *Proc. Canadian Workshop on Inf. Theory*, May 2009, pp. 165–168.

- [11] F. Simoens, H. Wymeersch, H. Steendam, and M. Moeneclaey, *Synchronization for MIMO systems*. Hindawi Publishing, 2005.
- [12] F. Bøhagen, P. Orten, and G. E. Øien, "Design of optimal high-rank line-of-sight MIMO channels," *IEEE Trans. Wireless Commun.*, vol. 4, no. 6, pp. 1420–1425, Apr. 2007.
- [13] Y. Wang and D. Falconer, "Phase noise estimation and suppression for single carrier SDMA uplink," in *Proc. IEEE Wireless Commun. and Networking Conf.*, Jul. 2010.
- [14] N. Hadaschik *et al.*, "Improving MIMO phase noise estimation by exploiting spatial correlations," in *Proc. IEEE Int. Conf. on Acoustics, Speech and Signal Process.*, 2005, pp. 833–836.
- [15] A. A. Nasir, H. Mehrpouyan, R. Schober, and Y. Hua, "Phase noise in MIMO systems: Bayesian Cramer-Rao bounds and soft-input estimation," *IEEE Trans. Signal Process.*, vol. 61, no. 10, pp. 2675–2692, May 2013.
- [16] A. Demir, A. Mehrotra, and J. Roychowdhury, "Phase noise in oscillators: a unifying theory and numerical methods for characterization," *IEEE Trans. Circuits Syst.*, vol. 47, no. 5, pp. 655–674, May 2000.
- [17] S. M. Kay, *Fundamentals of Statistical Signal Processing, Estimation Theory*. Prentice Hall, Signal Processing Series, 1993.
- [18] A. Hajimiri, S. Limotyrakis, and T. H. Lee, "Jitter and phase noise in ring oscillators," *IEEE J. Solid-State Circuits*, vol. 34, no. 6, pp. 790–804, Jun. 1999.
- [19] J. Boutros, F. Boixadera, and C. Lamy, "Bit-interleaved coded modulations for multiple-input multiple-output channels," in *Proc. IEEE Int. Symp. Spread Spectrum Tech. and App.*, vol. 1, Sep. 2000, pp. 123–126.
- [20] I. Ziskind and M. Wax, "Maximum likelihood localization of multiple sources by alternating projection," *IEEE Trans. Acoust., Speech, Signal Process.*, vol. 36, no. 10, pp. 1553–1560, Oct. 1988.
- [21] "Goddard technical standard: Low density parity check code for rate 7/8," NASA Goddard Space Flight Center, Tech. Rep. GSFC-STD-9100.